New Zealand Journal of Geology and Geophysics

ISSN: 0028-8306 (Print) 1175-8791 (Online) Journal homepage: http://www.tandfonline.com/loi/tnzg20

Petrology of metabasalts from the Chrystalls Beach accretionary mélange - implications for tectonic setting and terrane origin

Åke Fagereng & Alan F. Cooper

To cite this article: Åke Fagereng & Alan F. Cooper (2010) Petrology of metabasalts from the Chrystalls Beach accretionary mélange - implications for tectonic setting and terrane origin, New Zealand Journal of Geology and Geophysics, 53:1, 57-70, DOI: 10.1080/00288301003631806

To link to this article: http://dx.doi.org/10.1080/00288301003631806

Published online: 14 Apr 2010.

Submit your article to this journal

Article views: 553

View related articles

Citing articles: 6 View citing articles

Full Terms & Conditions of access and use can be found at
http://www.tandfonline.com/action/journalInformation?journalCode=tnzg20

Download by: [203.118.170.61] **Date:** 24 February 2017, At: 22:27

New Zealand Journal of Geology and Geophysics
Vol. 53, No. 1, March 2010, 57–70

Routledge
Taylor & Francis Group

Petrology of metabasalts from the Chrystalls Beach accretionary mélange - implications for tectonic setting and terrane origin

Åke Fagereng* and Alan F. Cooper

Department of Geology, University of Otago, Dunedin, New Zealand

(*Received 13 October 2009; final version received 8 December 2009*)

The Chrystalls Beach Complex is interpreted as an accretionary mélange within the Otago Schist on the South Island of New Zealand. Its stratigraphic position within the New Zealand Mesozoic accretionary prism is not well constrained, and the terrane affinity of the complex has remained enigmatic. Previous studies have focused on age relationships and sediment geochemistry. In this contribution we present geochemical data for metabasalts within the complex. Two distinctly different basalt compositions are found in the mélange. Metabasalts outcropping at the northern end of the complex have an inferred mid-ocean ridge affinity, while metabasalts in the central part of the assemblage are suggested to represent ocean island basalts. It is speculated that the northern mid-ocean ridge basalts represent blocks from the crust of a subducting slab, while the ocean island basalts are part of a subducting seamount. These tectonic affinities are in agreement with mélange formation during subduction of material below the Otago Schist protolith. In this setting, the mélange may contain material derived from both the Caples and Rakaia Terranes, or represent a different terrane fragment.

Keywords: basalt; melange; subduction; accretionary prism; Otago Schist; Chrystalls Beach Complex

Introduction

The Otago Schist forms a 160 km wide belt of deformed and metamorphosed greywacke, shale, chert, and basalt (Fig. 1; Mortimer 1993a, b, 2000; Turnbull 2000) in the southern South Island of New Zealand. The schist has been interpreted as a deeply exhumed section of a Late Paleozoic-Mesozoic accretionary prism, formed by subduction under the paleo-Pacific Gondwana margin (Coombs et al. 1976; Wood 1978; MacKinnon 1983; Korsch & Wellman 1988; Mortimer 1993a, b, 2003; Breeding & Ague 2002). Peak metamorphic temperatures have been estimated in the range 350–400°C (Yardley 1982; Mortimer 2000). The metamorphic overprint predominantly affects the sedimentary Caples and Rakaia (older Torlesse) Terranes. The Caples/Rakaia terrane boundary is a suture zone defined geochemically along the core of the Otago Schist belt (Roser & Cooper 1990; Mortimer & Roser 1992; Mortimer 1993a).

The Chrystalls Beach Complex, an accretionary mélange in southeast Otago (Fig. 1) (Nelson 1982), is not well correlated with other terranes within the Otago Schist (Mortimer & Roser 1992; Roser et al. 1993; Adams & Graham 1997; Landis et al. 1999; Coombs et al. 2000). The complex is bounded by the Rakaia Terrane to the north and the Caples Terrane to the west, and is thought to represent either an atypical part of the Caples Terrane or a separate entity with a different history from surrounding terranes (Coombs et al. 2000).

The Complex comprises lenses of greywacke, chert, and minor basalt enclosed in a cleaved pelitic matrix (Robinson 1958; Nelson 1982) and has experienced stratal disruption typical of mélange shear zones (Nelson 1982). Radiolarian fossils (Campbell & Campbell 1970; Aita & Bragin 1999) and detrital zircon ages (Adams et al. 2007) indicate an Early-Late Triassic protolith age. Graphitisation and K-Ar ages indicate a progressive metamorphic gradient with increasing grade of metamorphism from south to north in the complex, with peak metamorphic ages in the Middle-Late Jurassic (Nishimura et al. 2000). Metamorphic assemblages and mineral chemistry indicate peak pressure-temperature conditions of <600 MPa and <300°C (Å. Fagereng unpublished data; Nishimura et al. 2000).

This paper explores the petrography and geochemistry of Chrystalls Beach Complex metabasalts in order to compare these rocks to subduction-related assemblages elsewhere in the world. New whole-rock and mineral geochemical data and petrographic descriptions of rocks from the Chrystalls Beach Complex are presented, with the aim of constraining the geological history of the complex.

Methods

Sample locations and mineralogy are listed in Table 1. The samples were cleaned, trimmed of weathered crust, and crushed in a tungsten-carbide swing-mill until a fine powder was obtained. Whole-rock powders were analysed for major

*Corresponding author. Email: ake@geology.co.nz

ISSN 0028-8306 print/ISSN 1175-8791 online
© 2010 The Royal Society of New Zealand
DOI: 10.1080/00288301003631806
http://www.informaworld.com

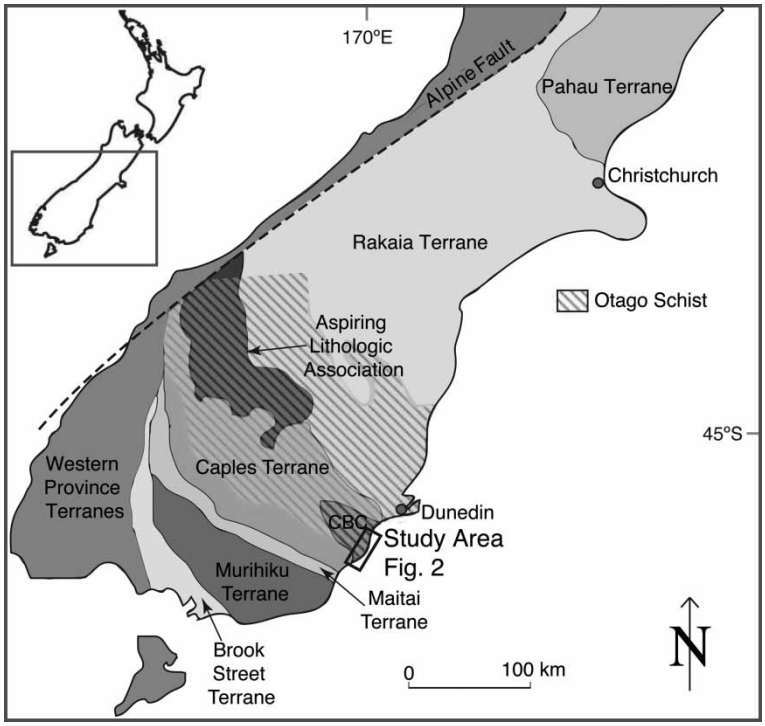

Fig. 1 Location of the Otago Schist and the Chrystalls Beach Complex in the South Island of New Zealand. Geology after Mortimer (1993b).

elements by X-ray fluorescence (XRF) in the Department of Geology, University of Otago and for minor and rare-earth elements (REE) by Laser Ablation-Inductively Coupled Plasma-Mass Spectrometry (LA-ICP-MS) in the Centre for Trace Element Analysis, University of Otago. Both major and minor elements were analysed in fused discs. LA-ICP-MS analyses used a laser frequency of 10 Hz and spot size of 100 μm, ablating the fused disc along a line 200 μm long at a speed of 5 μm/s. Data were standardised using a lithium-borate silica glass standard (NIST-610).

Semi-quantitative mineral chemistry was determined by energy dispersive spectrometry (EDS) using a JEOL

Table 1 Location, short description, and mineralogy of metabasalt samples. Mineralogy determined from XRD and thin section study. Mineral abbreviations following Bucher & Frey (2002) (see Fig. 2 for sample locations)

Location	Sample	E	N	Short sample description	Mineralogy
Watsons Beach	OU77461	2289810	5445560	Chloritised and sericitised albite-phyric basalt	Chl + Ab + Ms + Pmp ± Ep ± Qtz ± Cpx
	OU77462	2288775	5444435	Chloritised and sericitised albite-phyric basalt	Ab + Chl + Pmp ± Ms ± Ep
Akatore Creek	OU77463	2291670	5451747	Microcrystalline vesicular (chlorite-filled) basalt	Chl + Ms + Ab ± Hem ± Ttn ± Ep
	OU77464	2291777	5451651	Microcrystalline vesicular (chlorite-filled) basalt	Chl + Ms + Ab ± Ep ± Ttn
	OU77465	2291777	5451651	Chloritised microcrystalline basalt	Chl + Ms + Ab ± Ep ± Qtz
	OU77466	2291777	5451651	Chloritised seriate-textured basalt	Ab + Chl + Ms ± Ep ± Ttn
	OU77470	2292282	5450765	Microcrystalline basalt	Chl + Ms + Ab ± Ep ± Cal ± Hem
	OU77473	2292145	5448445	Variolitic microcrystalline basalt	Chl + Ms + Ab ± Ep ± Ttn
	OU77474	2292241	5448725	Variolitic microcrystalline pillow basalt	Ab + Chl + Act ± Ep ± Ms ± Ttn
	OU77475	2292241	5448725	Variolitic microcrystalline pillow basalt	Ab + Chl + Ms + Act ± Ep ± Ttn
	OU77476	2292317	5449201	Porphyritic amygdaloidal basalt	Ab + Chl + Ms ± Stp ± Ep ± Cal ± Act
Taieri Mouth	OU77478	2293330	5456500	Microcrystalline pillow basalt	Ms + Chl + Ab ± Ep ± Act ± Cpx
	OU77479	2293330	5456500	Microcrystalline pillow basalt	Chl + Ms + Ab + Cpx + Pmp ± Ep ± Act
	OU77480	2293330	5456500	Microcrystalline pillow basalt	Chl + Ab + Ms + Cpx ± Ep ± Act

JXA-8600 electron probe micro-analyser (EPMA) housed in the Department of Geology, University of Otago. Analyses were performed on carbon-coated polished thin sections, with beam conditions of 15 kV and 1 nA, beam diameter of 20 μm, and 200 s live counting time, with natural and synthetic minerals and oxides as standards.

Field relations and petrography

Nelson (1982) divided the lithologies of the Chrystalls Beach Complex into two main units: a sandstone-shale association and a volcanogenic association. The former is predominant (>90% by area) and consists of a dismembered sequence of interbedded sandstone and grey/black mudstone. The latter comprises varicoloured chert and mudstone, basalts, and black radiolarian chert (Nelson 1982). Fragments (long dimension of centimetres to tens of metres) of the volcanogenic association occur within sandstone-shale association rock assemblages and vice-versa (Nelson 1982; Hada et al. 1988). The rocks exhibit mixed continuous-discontinuous deformation features typical of block-in-matrix mélange, and no primary stratigraphic sequence has been determined (Nelson 1982; Hada et al. 1988).

Only c. 1% of the Chrystalls Beach Complex comprises outcrop of coherent metabasalt (Nelson 1982; Hada et al. 1988). Apart from two small units of relatively massive, green, metabasalt south of Watsons Beach (Figs. 2, 3A), these outcrops are situated in the northern part of the complex. Two large (>100 m across) blocks of purple metabasalt are present: one south of Akatore Creek and one at Taieri Mouth. The Taieri Mouth block is bounded by the Akatore Fault to the northwest and obscured by beach sand to the south. The large Akatore Creek metabasalt block is fault-bounded on both exposed sides. Smaller, massive, metabasalt units occur in sedimentary, olistostromal, or tectonic contact with surrounding mélange (Figs. 3B, C). These smaller blocks are petrographically distinguishable from each other and, as mapped by Nelson (1982), likely represent separate units. Near the contact between metabasalt and surrounding sediments there is often a degree of hydrothermal alteration and apparent soft-sediment mixing of units (Fig. 3C). Breccias and volcanogenic association varicoloured mudstones are common near and within metabasalt units (Figs. 3D, E) and usually separate these from sandstone-shale association mélange. These breccias contain abundant volcanic fragments and are interpreted as volcanic breccias. The varicoloured mudstones contain amorphous material, are rich in silica relative to grey mudstones (Å. Fagereng unpublished data), and with their close association to metavolcanic rocks are interpreted as metatuffs. Remnant pillow structures are preserved in the large metabasalt blocks near Akatore

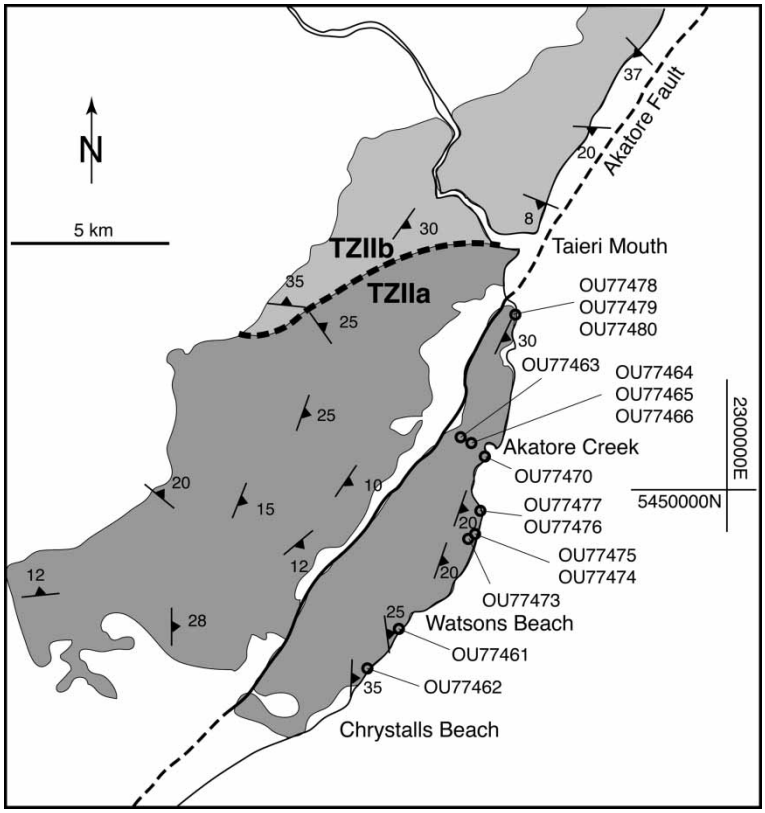

Fig. 2 Simple geological map of the Chrystalls Beach Complex after Bishop (1994) and Bishop & Turnbull (1997), showing sample locations for the current study. Grid references are New Zealand map grid. See Fig. 1 for the location of this figure.

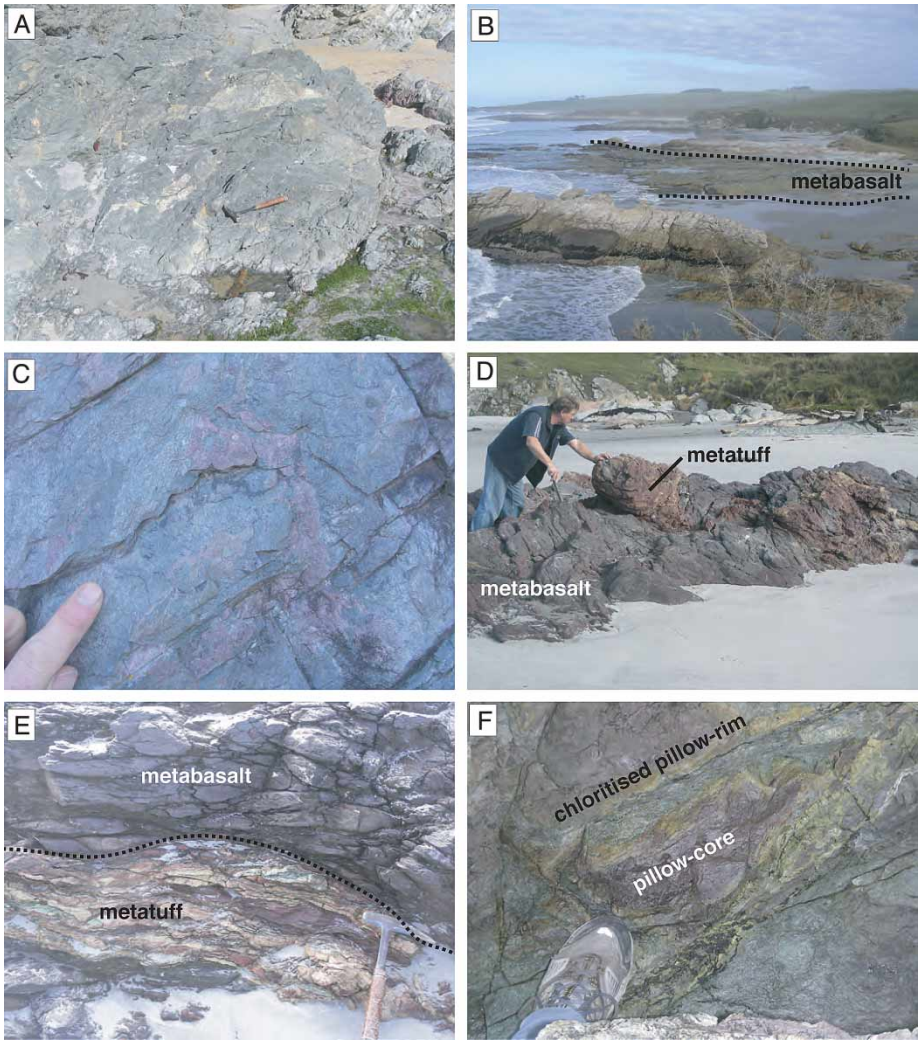

Fig. 3 Photographs of metabasalt in outcrop: (A) massive green metabasalt near Watsons Beach; (B) block of metabasalt within sandstone-shale melange, south of Akatore Creek; (C) mixing of purple and green, massive metabasalts, Akatore Creek; (D) interbedded massive basalt and layered tuff, south of Akatore Creek; (E) close-up of basalt-tuff contact in (D); (F) stretched purple metabasalt pillow surrounded by a chloritised alteration rim, south of Akatore Creek.

Creek and Taieri Mouth (Fig. 3F), which indicates these metabasalts originated as pillow lava. Where recognisable, pillows are generally well preserved although commonly stretched to an ellipsoidal shape (Fig. 3F) and pillow rims are commonly altered to chlorite-rich assemblages (Fig. 3F).

Watsons Beach

The two massive, green metabasalt blocks south of Watsons Beach are c. 10–20 m across (Fig. 3A), crosscut by veins, and significantly altered. Both are blocks in a mélange matrix and likely a substantial distance from their place of deposition. Microscopically, both units appear similar with subhedral to euhedral phenocrysts of plagioclase feldspar in a microcrystalline matrix of plagioclase, epidote, muscovite, chlorite, pumpellyite, and opaque minerals (Fig. 4A; Table 1). A few relict clinopyroxene crystals are observed in sample OU77461. Plagioclase is almost 100% albite, an effect of metamorphic albitisation forming pseudomorphs after a plagioclase solid solution. Muscovite and pumpellyite are mostly present as secondary minerals in veins, or replacing feldspar or volcanic glass. Epidote and chlorite are also present both in veins and as secondary matrix minerals, although which mineral(s) they have replaced is uncertain. Abundant calcite and minor isolated quartz veins cut these metabasalts.

Akatore Creek

Metabasalt is most abundant immediately south of Akatore Creek (Fig. 2). These outcrops contain massive purple metabasalt interbedded with varicoloured mudstone, and one larger fault-bounded block of metabasalt with preserved

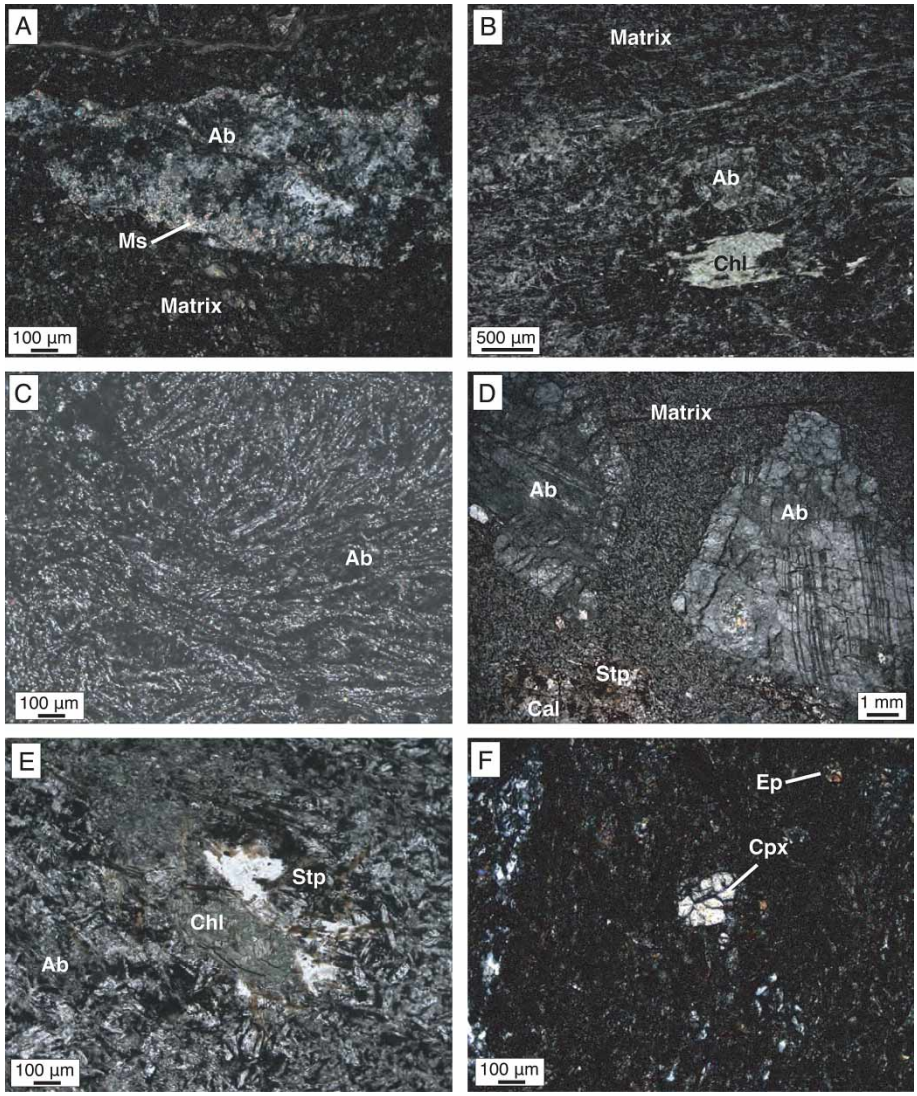

Fig. 4 Photomicrographs of metabasalts from the Chrystalls Beach Complex: (A) subhedral plagioglase phenocryst partly replaced by white mica, Watsons Beach (OU77461, XPL); (B) chlorite-filled vesicle in microcrystalline matrix, Akatore Creek (OU77463, PPL); (C) variolitic texture displayed by plagioclase laths, Akatore Creek (OU77475, XPL); (D) sub- to euhedral plagioclase phenocrysts and stilpnomelane + calcite filled amygdale in a microcrystalline matrix, Akatore Creek (OU77477, XPL); (E) close-up of stilpnomelane and chlorite amygdale within a microcrystalline plagioclase matrix, Akatore Creek (OU77476, PPL); (F) clinopyroxene in microcrystalline plagioclase-white mica-epidote matrix, Taieri Mouth (OU77480, XPL).

pillow structures. Petrographically there appears to be at least two different units of massive metabasalt. However, as these blocks are within a mélange, their relationship to each other is impossible to determine with any certainty. The massive metabasalts are commonly microcrystalline and, in places, extensively chloritised (Fig. 4B; Table 1). The major minerals are albite and chlorite. Albite is extensively altered to sericite, so that the matrix is made up of albite and muscovite with secondary epidote, minor titanite, and opaque minerals. Chlorite is mostly present filling vesicles and in localised veins. Quartz and calcite occur locally in veins.

Variolitic texture is common in pillow basalts but was only observed in one massive basalt (Table 1). This texture is caused by radial orientation of plagioclase laths, sometimes altered to sericite (Fig. 4C). Epidote, actinolite, and chlorite are present as secondary metamorphic minerals in these rocks.

A massive porphyritic metabasalt crops out at a location south of Akatore Creek (samples OU77476, OU77477; Fig. 2). In this rock, euhedral phenocrysts of albite are present in a matrix of albite, muscovite, chlorite, actinolite, and epidote (Fig. 4D). Stilpnomelane, chlorite, and calcite fill what is inferred to be amygdales, with elongated stilpnomelane crystals extending from the amygdale edge into a centre of chlorite and/or calcite (Fig. 4E). Chlorite and actinolite also form scattered pseudomorphs of either

a completely replaced phenocryst phase (likely olivine) or vesicles.

Taieri Mouth

Another large block of pillow basalt occurs at Taieri Mouth. This unit is microcrystalline and contains relatively equigranular plagioclase, epidote, clinopyroxene, and minor actinolite (Fig. 4F). Feldspar is extensively albitised and sericitised. Chlorite is present; mostly filling what appears to have been vesicles in the original lava deposit or pseudomorphs after anhedral olivine or glass. Vein minerals include quartz, calcite, epidote, chlorite, and minor pumpellyite. Pumpellyite is also present as a minor secondary phase replacing feldspar.

Clinopyroxene composition

The basaltic rocks in the Chrystalls Beach Complex are extensively altered, and few primary minerals are preserved. Clinopyroxene is generally considered resistant to alteration (e.g., Nisbet & Pearce 1977; Leterrier et al. 1982; Shervais & Kimbrough 1985), but is only observed in pillow basalts at Taieri Mouth and in one altered basalt block at Watsons Beach. Average clinopyroxene compositions are listed in Table 2. In a Mg-Fe-Ca triangular diagram, the clinopyroxenes plot in a relatively tight cluster at the Ca-rich limit of the augite field (Fig. 5A).

Because they are considered resistant to alteration during low-grade metamorphism, clinopyroxene compositions can be used to determine tectonic affiliation. In a Si-Na-Ti trivariant diagram (after Beccaluva et al. 1989), the clinopyroxenes plot in the field of mid-ocean ridge basalts although overlapping with the ocean island basalt field (Fig. 5B). Using the F1-F2 discriminant functions of Nisbet & Pearce (1977), the clinopyroxenes again plot in the mid-ocean ridge basalt field; however, here they cannot be distinguished from island arc basalts (Fig. 5C).

Leterrier et al. (1982) designed discriminant diagrams to distinguish between sub-alkaline and alkaline basalts, and non-orogenic and orogenic basalts. The clinopyroxenes from the Chrystalls Beach Complex plot as sub-alkaline (Fig. 5D) and non-orogenic (Fig. 5E) in these diagrams, although some Watsons Beach analyses plot in the overlap of the orogenic and non-orogenic fields.

Whole-rock composition

Whole-rock XRF and LA-ICP-MS analyses of major and minor elements are presented in Table 3. Loss on ignition is relatively high in all samples and, as with all very low-grade metamorphic rocks, element mobility is a considerable problem. As the rocks have undergone significant alteration, only relatively immobile elements are considered when attempting to classify these basalts.

Table 2 Average chemical compositions of clinopyroxenes in Chrystalls Beach Complex metabasalts. Calculations are based on 6 oxygens, all Fe as Fe^{2+}, S.D. = standard deviation, n = number of samples

Sample	OU77461		OU77479		OU77480	
n =	5	S.D.	8	S.D.	10	S.D.
SiO_2	51.16	0.88	51.03	1.27	48.88	0.94
TiO_2	0.75	0.11	0.87	0.30	1.30	0.34
Al_2O_3	1.90	0.73	4.24	1.57	4.91	0.76
Cr_2O_3	0.08	0.09	0.31	0.19	0.20	0.12
FeO	8.60	0.85	7.35	0.30	8.03	0.90
MnO	0.30	0.13	0.20	0.07	0.22	0.05
MgO	15.88	0.59	16.39	1.95	15.05	0.88
CaO	19.35	0.68	18.51	1.91	19.02	0.90
Na_2O	0.14	0.06	0.54	1.18	0.34	0.20
K_2O	0.06	0.03	0.06	0.05	0.10	0.15
Total	98.22	0.58	99.50	0.56	98.05	0.64
Si	1.93	0.02	1.89	0.04	1.85	0.03
Ti	0.02	0.00	0.02	0.01	0.04	0.01
Al	0.08	0.03	0.18	0.07	0.22	0.03
Cr	0.00	0.00	0.01	0.01	0.01	0.00
Fe	0.27	0.03	0.23	0.01	0.25	0.03
Mn	0.01	0.00	0.01	0.00	0.01	0.00
Mg	0.89	0.03	0.90	0.10	0.85	0.05
Ca	0.78	0.03	0.73	0.08	0.77	0.03
Na	0.01	0.00	0.04	0.08	0.02	0.01
K	0.00	0.00	0.00	0.00	0.00	0.01

A plot of Zr/Ti against Nb/Y is used to classify the rocks by alkalinity and stage of differentiation (Fig. 6) (Winchester & Floyd 1977; Pearce 1996). In this diagram, the Chrystalls Beach Complex basalts plot in three distinct groups, equivalent to the three groups determined by sampling locality. Taieri Mouth and Watsons Beach basalts both plot in the sub-alkaline part of the basalt field, with Taieri Mouth samples notably less alkaline than those from Watsons Beach. Samples from Akatore Creek, on the other hand, plot in both basalt and alkali basalt fields, and are thus significantly more alkaline than the other samples. Note that the different basalts in the Chrystalls Beach Complex are discriminated (in Fig. 6) by a different degree of alkalinity (i.e., Nb/Y ratio), and are all at a similar stage of differentiation (i.e., similar Zr/Ti ratio).

To discriminate between different tectonic environments, basalt compositions were plotted in a number of discrimination diagrams (Fig. 7). Basalt tectonic environments are commonly determined as either mid-ocean ridge (MORB), island arc (IAB), or ocean island (OIB). This analysis is aimed at discriminating between these three environments for each of the three groups of basalt in the Chrystalls Beach Complex.

Figure 7A shows a Zr/Y versus Zr plot after Pearce & Norry (1979). Akatore Creek basalts all plot in the OIB field, Taieri Mouth samples plot as MORB, while Watsons Beach samples fall in the overlap between the MORB and IAB fields. The Ti-V diagram of Shervais (1982) can be used to distinguish IAB and MORB (Fig. 7B). In this diagram Taieri Mouth rocks still plot in the MORB field, while Akatore Creek basalts plot in both OIB and MORB fields. Watsons Beach basalts fall within the MORB field but overlap with the most Ti-poor samples from Akatore Creek.

Figures 7A and B are classical plots much used in the literature. A recent review of basalt tectonic discrimination diagrams by Vermeesch (2006) found new discrimination diagrams based on statistical analyses of a large dataset of basalts of known tectonic affinity. In this review, a Sm-Ti-V

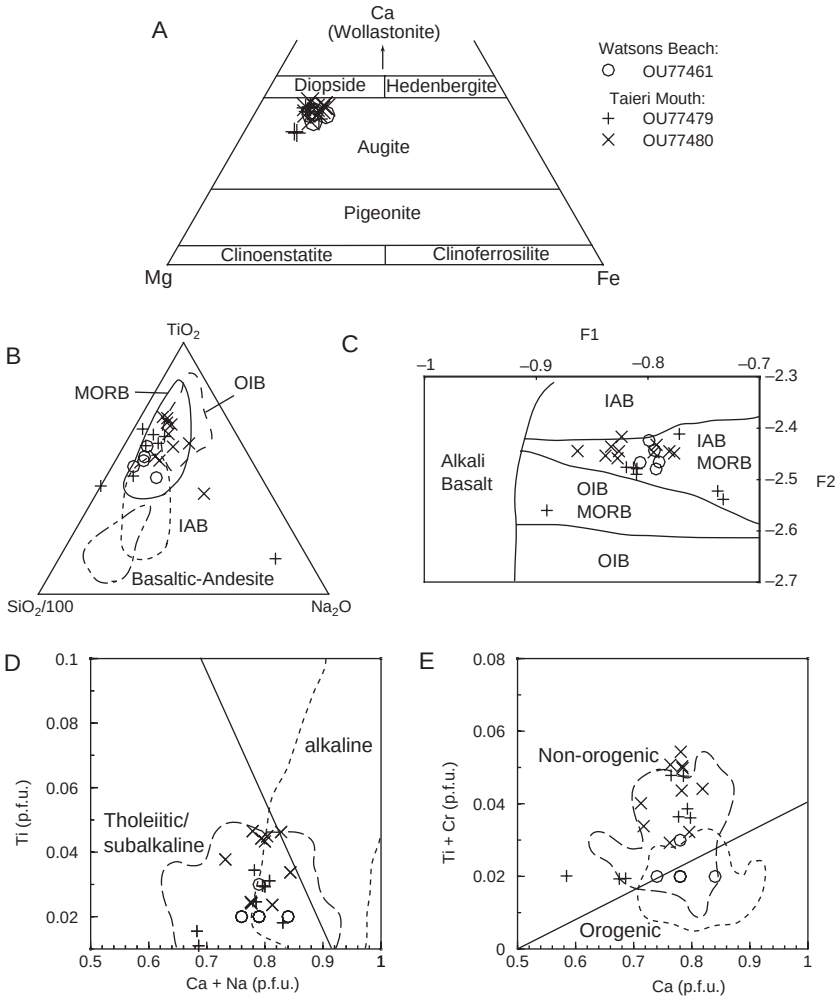

Fig. 5 Clinopyroxene compositions: (A) clinopyroxene classification diagram (Morimoto 1988); (B) tectonic discrimination diagram, after Beccaluva et al. (1989); (C) plot of discriminant functions, following Nisbet & Pearce (1977); (D), (E) clinopyroxene discrimination diagrams after Leterrier et al. (1982).

Table 3 Major and minor element composition of Chrystalls Beach Complex metabasalts. See Table 1 and Fig. 2 for sample details and locations (total Fe as Fe_2O_3; LOI: loss on ignition; bdl: below detection limit)

	Watsons Beach		Akatore Creek									Taieri Mouth		
Sample	OU77461	OU77462	OU77463	OU77464	OU77465	OU77466	OU77470	OU77473	OU77474	OU77475	OU77476	OU77478	OU77479	OU77480
SiO_2	40.79	47.95	45.47	45.54	43.37	44.15	47.29	47.55	48.61	48.60	49.05	46.41	47.91	48.27
TiO_2	1.51	1.67	2.78	3.02	3.23	2.99	1.58	2.37	2.43	2.44	2.88	1.93	1.87	1.82
Al_2O_3	18.08	18.26	19.81	18.64	18.30	17.76	16.04	16.48	16.49	17.16	16.92	16.67	15.66	15.36
$Fe_2O_3^t$	12.64	10.38	13.65	12.12	12.35	11.10	10.23	11.70	12.43	11.90	14.83	14.02	13.56	13.15
MnO	0.74	0.21	0.07	0.14	0.16	0.16	0.28	0.13	0.10	0.11	0.15	0.18	0.24	0.22
MgO	6.45	6.10	1.96	5.00	7.13	7.84	5.86	3.41	3.60	3.90	1.96	3.09	5.58	5.47
CaO	9.54	6.44	5.51	5.74	5.58	6.88	6.60	9.07	7.42	6.26	3.76	9.19	7.80	8.35
Na_2O	2.59	3.91	2.93	3.32	3.07	2.85	5.34	3.21	4.16	3.93	4.59	3.03	2.95	2.96
K_2O	0.53	0.47	3.39	1.30	1.02	0.76	0.30	1.40	1.05	1.93	2.70	1.55	1.46	1.36
P_2O_5	0.17	0.17	0.58	0.54	0.54	0.48	0.24	0.29	0.35	0.39	0.54	0.22	0.20	0.20
LOI	8.58	4.28	2.88	4.14	4.81	4.51	6.60	4.04	2.72	2.90	2.31	3.20	2.83	2.76
Total	101.62	99.84	99.03	99.50	99.56	99.48	100.36	99.65	99.36	99.52	99.69	99.49	100.06	99.92
V	298	277	288	299	303	287	283	357	362	344	318	304	360	340
Cr	165	114	189	227	251	238	448	293	312	298	41	154	147	145
Co	48	50	34	51	52	51	53	55	54	46	51	64	69	63
Ni	65	69	100	153	175	172	134	100	111	114	59	72	75	68
Ga	18	16	23	21	22	20	16	19	19	20	23	19	19	17
Rb	18	16	54	24	21	17	10	37	27	54	88	27	26	24
Sr	164	211	491	360	359	358	80	276	140	189	191	159	122	120
Y	26.5	23.0	32.9	34.8	32.5	30.6	23.3	33.9	38.9	37.5	42.3	38.0	36.9	36.2
Zr	89	97	212	233	255	235	111	172	179	180	196	108	108	101
Nb	4.3	5.8	26.9	30.0	32.1	30.3	13.9	18.8	19.3	19.5	22.2	2.9	2.5	2.6
Cs	2.0	1.3	9.2	3.5	1.7	1.7	0.5	3.8	2.2	3.9	6.6	1.6	1.3	1.3
Ba	59	79	360	204	163	101	67	161	132	252	355	116	129	105
La	11.6	12.5	35.4	37.5	36.6	38.7	19.5	23.8	24.7	24.6	28.1	11.0	10.3	13.8
Ce	12.1	15.7	61.9	63.4	66.2	55.5	31.3	38.9	39.2	41.5	50.3	14.2	13.2	12.9
Pr	2.0	2.1	8.3	8.4	8.7	7.6	4.0	5.0	5.4	5.8	6.8	2.7	2.3	2.3
Nd	9.6	12.0	34.7	37.2	36.1	28.9	17.5	23.7	25.5	27.5	30.6	15.4	11.7	11.2
Sm	2.9	3.4	7.8	8.4	8.9	7.4	4.5	5.9	6.3	6.9	6.5	4.8	4.8	5.0
Eu	1.0	1.0	2.7	2.3	2.5	2.2	1.4	2.1	2.2	2.3	2.3	1.8	1.6	1.7
Gd	4.3	4.4	7.5	7.5	7.9	6.1	3.6	7.0	7.9	7.1	6.6	6.4	5.1	5.2
Tb	0.8	0.7	1.1	1.3	1.3	1.4	0.8	0.9	1.3	1.2	1.2	1.1	1.1	1.1
Dy	5.3	4.5	6.8	8.1	8.0	6.4	4.8	6.5	7.5	6.6	7.8	7.4	7.2	6.2
Ho	0.9	0.9	1.4	1.1	1.4	1.3	1.1	1.4	1.4	1.3	1.7	1.6	1.4	1.4
Er	2.4	2.9	3.3	3.5	4.1	3.4	2.6	3.8	4.0	4.0	4.8	4.5	4.0	4.0
Tm	0.5	0.5	0.6	0.7	0.6	0.5	0.3	0.4	0.5	0.5	0.5	0.6	0.6	0.6
Yb	2.6	2.1	3.3	3.7	3.7	3.5	2.8	3.8	3.7	3.6	4.5	3.6	3.6	3.6
Lu	0.5	0.2	0.3	0.6	0.7	0.4	0.3	0.4	0.5	0.5	0.4	0.6	0.6	0.5
Hf	2.3	1.8	5.5	5.7	5.8	6.2	2.4	3.8	5.1	3.9	4.8	3.0	2.9	2.5
Ta	0.4	0.4	1.8	1.9	2.0	1.6	0.7	1.0	1.4	1.2	1.3	0.3	0.1	0.2
Th	0.4	1.9	2.1	3.4	3.4	2.9	1.3	1.8	2.2	2.0	2.0	0.2	bdl	0.4
U	0.4	bdl	0.7	1.3	0.8	0.8	0.4	0.6	bdl	bdl	0.6	bdl	0.3	0.2

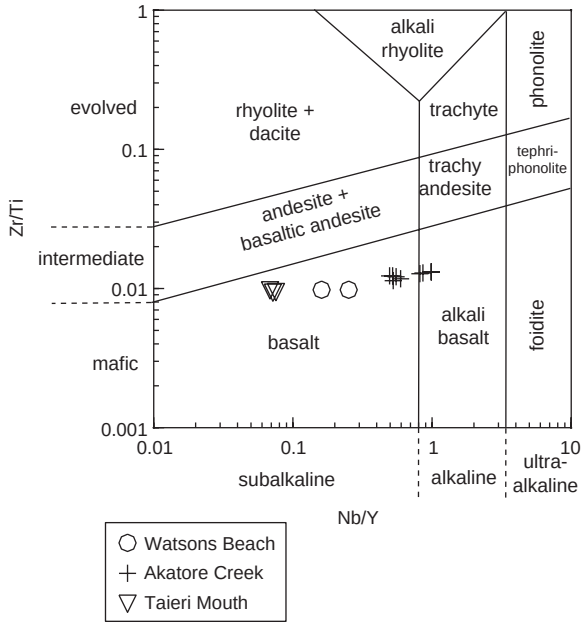

Fig. 6 Volcanic rocks in the Chrystalls Beach Complex plotted in the classification diagram of Winchester & Floyd (1977), revised by Pearce (1996). The diagram shows that, as determined petrographically, the rocks are basalts but plot in three distinct groups matching the three sampling localities.

ternary diagram was found to be the best quadratic discrimination diagram using only relatively immobile elements (Vermeesch 2006). Plotting Chrystalls Beach basalts in a Sm-Ti-V diagram (Fig. 7C) again suggests that the Taieri Mouth basalt block is a MORB. Akatore Creek samples plot in the overlap between MORB and OIB, although mostly in the OIB field. Watsons Beach basalts are identified as MORB in this plot (Fig. 7C).

While the discrimination diagrams in Fig. 7 only account for two or three elements each, spider diagrams (Fig. 8) show the general pattern of trace- and rare earth elements in each sample. Because this study considers altered, low-grade metamorphic rocks, mobile elements are omitted from these diagrams, leaving rare earth and high field strength elements.

Normalised to N-MORB (Fig. 8, left column), both Watsons Beach and Taieri Mouth basalts show relatively flat multi-element patterns, close to a 1:1 ratio over MORB. Enrichment in La and Th is observed in samples from both Watsons Beach and Taieri Mouth, which could be interpreted as signs of an evolved MORB source. Ta and Nb, however, are relatively low (near MORB values) in both of these localities, suggesting a normal MORB protolith which has experienced enrichment of La and Th during metasomatism. Akatore Creek samples are distinctly different from Watsons Beach and Taieri Mouth basalts. Strong enrichment in Th, Ta, and other high field strength elements relative to MORB is evident in the multi-element pattern

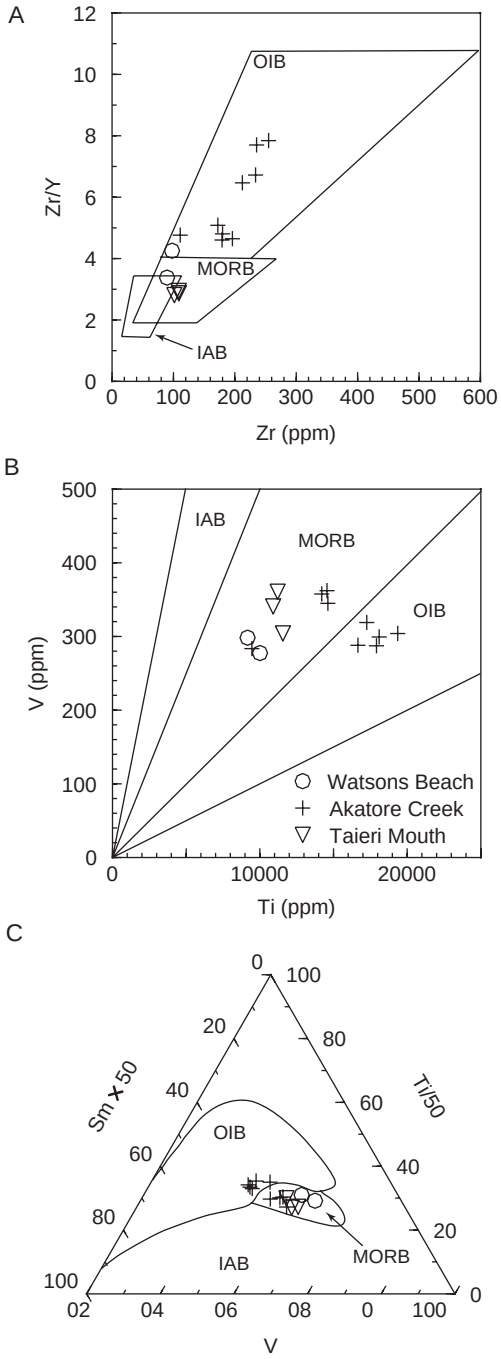

Fig. 7 Discrimination diagrams for Chrystalls Beach metabasalts.

of Akatore Creek Basalt and typical of OIB (Sun & McDonough 1989).

REE-patterns also show a similarity between Watsons Beach and Taieri Mouth basalts (Fig. 8, right column). The samples from these two locations have flat REE-patterns typical of N-MORB, although a very slight enrichment in light-REE in Watsons Beach samples may indicate an evolved (E-MORB) component. Slight depletion in Ce likely

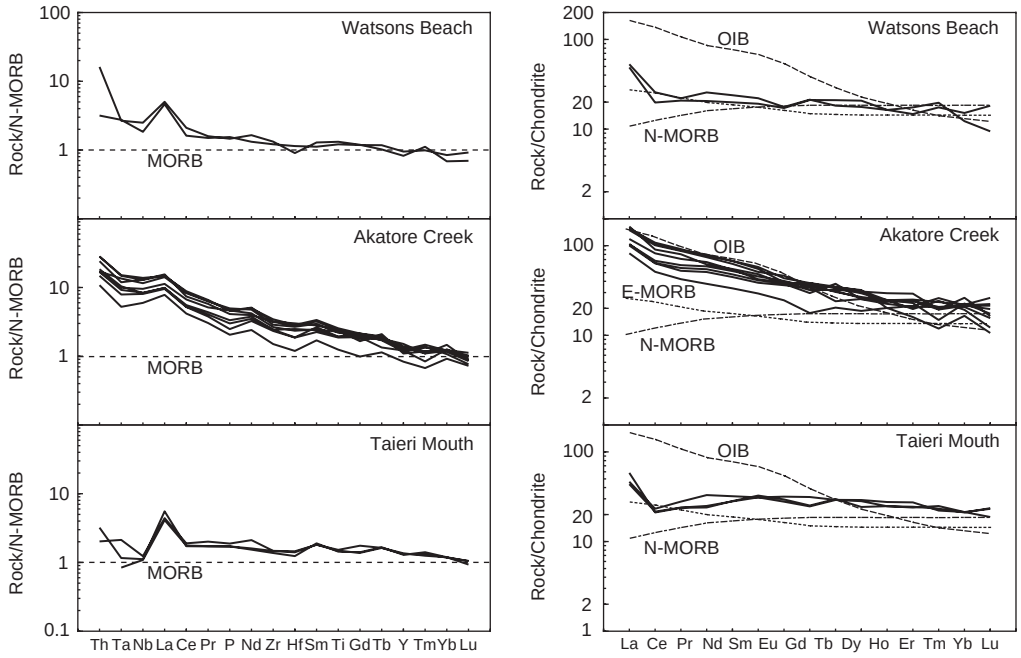

Fig. 8 Geochemistry of Chrystalls Beach metabasalts. Left column: multi-element pattern normalised to average mid-ocean ridge basalt. Right column: REE-pattern normalised to chondrite. Normalising values and typical OIB, N-MORB, and E-MORB compositions from Sun & McDonough (1989).

relates to sea-floor alteration (e.g., Ludden & Thompson 1979). Basalts from Akatore Creek show a strong enrichment ($>100 \times$Chondrite) in light-REE, again a typical feature of OIB (Sun & McDonough 1989).

Tectonic affinity

At least two different basalt compositions are present in the Chrystalls Beach Complex. Petrographically, Akatore Creek basalts are mostly microcrystalline although some are porphyritic with phenocrysts of albite and chlorite (pseudomorphs after Ca-plagioclase, olivine and/or pyroxene, respectively). Amygdales are common and filled with secondary chlorite, calcite, quartz, and stilpnomelane. Geochemically, these basalts are consistently classified as relatively alkaline high-TiO_2 OIB (Fig. 7). Remnant pillow structures, in basalts interbedded with radiolarian chert, indicate that at least some of the Akatore Creek OIB was emplaced in a submarine setting.

Pillow basalts at Taieri Mouth also have a microcrystalline matrix but lack the albite phenocrysts observed at Akatore Creek. Relict clinopyroxene is relatively common at Taieri Mouth, and the clinopyroxene compositions indicate a MORB affinity. Chemically, these pillow basalts are classified as sub-alkaline and consistently plot in the MORB field on whole-rock discrimination diagrams (Fig. 7). Trace- and REE-patterns are also compatible with a mid-ocean ridge environment (Fig. 8). It is very likely that the Taieri Mouth metabasalts were erupted at a mid-ocean ridge in a significantly different setting to the Akatore Creek basalts. The Akatore Creek block may, however, represent a seamount surrounded by MORB.

At Watsons Beach, metabasalt occurs as two small, massive blocks within mélange. Alteration of plagioclase to albite, white mica, epidote, and pumpellyite, and an abundance of mineralised veins, indicates that these rocks were more pervasively altered than the Taieri Mouth and Akatore Creek basalts and are therefore more difficult to classify. Petrographically, the Watsons Beach basalts are similar to the basalts at Akatore Creek as they are also porphyritic with albite pseudomorphs in a microcrystalline matrix. In discrimination diagrams, the two Watsons Beach samples plot in a variety of tectonic fields, but show a general MORB affinity. In the diagram suggested by Vermeesch (2006) as the best discrimination diagram for basalt using immobile elements, Watsons Beach samples plot as MORB (Fig. 7C). The trace element and REE-patterns also indicate a mid-ocean ridge origin (Fig. 8). Clinopyroxene compositions are more resistant to alteration effects than whole-rock compositions. Clinopyroxene compositions in sample OU77461 from Watsons Beach are mostly indistinguishable from clinopyroxene compositions in Taieri Mouth basalts. The metabasalts at Watsons Beach are either a more enriched MORB (E-MORB) than the samples from Taieri Mouth, or more altered rocks from the same setting as the Taieri Mouth basalt unit.

Origin of the Chrystalls Beach Complex

In the geological history of the Otago Schist, it is proposed that the Rakaia Terrane sediments were derived from a continental volcanic arc and deposited in a trench environment at the Gondwana paleo-Pacific margin (MacKinnon 1983; Roser & Korsch 1999). The Rakaia sediments are then inferred to have been transported along a dextral margin-parallel strike-slip boundary and eventually amalgamated with the volcanogenic Caples Terrane in an accretionary wedge (e.g., MacKinnon 1983; Mortimer 1993b; Adams et al. 2007). During the Jurassic, both the Caples and the Rakaia Terrane were deformed and metamorphosed in the Rangitata Orogeny, leading to the formation of the Otago Schist (e.g., Coombs et al. 1976; Bradshaw et al. 1981; Mortimer 1993b, 2004; Adams & Graham 1997). Overall, the Mesozoic history of New Zealand has been interpreted as progressive growth by accretion at an obliquely convergent margin, where first the Caples and then the Rakaia were accreted onto the paleo-Pacific Gondwana coastline (see review by Mortimer 2004).

In this inferred geological history, the Chrystalls Beach Complex is suggested to have been incorporated into the Otago Schist during Jurassic subduction under the Gondwana margin (Adams & Robinson 1993; Adams & Graham 1997; Nishimura et al. 2000; Hada et al. 2001). The Chrystalls Beach Complex rock assemblage includes turbidity current deposits, volcanogenic deposits, radiolarian chert, and pillow basalts. This is equivalent to the lithologies observed in modern trench-fill deposits (Howell & Murray 1986; Hay et al. 1988; von Huene & Scholl 1991; Underwood 2007). Thus, as also noted previously by Nelson (1982) and Coombs et al. (2000), the lithological assemblage in the mélange is consistent with deposition in a trench followed by incorporation into an accretionary prism.

At the northernmost end of the mélange (Taieri Mouth), basalts show a distinct MORB affinity in both discrimination diagrams and trace-element patterns. Further south (Akatore Creek), at a slightly lower metamorphic grade, basalts of suggested OIB affinity have been sampled. Assuming that metamorphic grade is a measure of depth (Nishimura et al. 2000; Mortimer 2003), this indicates MORB pillow basalts near the base of the Complex overlain by blocks of OIB within mélange. The Akatore Creek basalts could therefore either represent exotic blocks from a distant ocean island or deposits from a subducted seamount related to the Chrystalls Beach Complex rock assemblage. The two small MORB-like blocks within mélange at Watsons Beach, at the highest structural level, could be fragments of oceanic crust broken off during collision and incorporated in the sediment pile on top of the subducting slab. The variation in composition from OIB-type to MORB-type basalts, as inferred here in the Chrystalls Beach Complex, has also been interpreted from dredge samples in a number of ocean basins (see collated data in Pearce 2008). There is therefore limited control on the distance between where OIB and MORB were initially emplaced.

Geometrically and geographically, the Chrystalls Beach Complex is situated between the Caples and Rakaia Terranes or alongside the Caples Terrane. Both the Caples and the Rakaia contain scattered basaltic rocks of varying composition (e.g., Mortimer 1993a; Turnbull 2000). Collating basalt analyses from throughout the Otago Schist would be a worthwhile future project, but is beyond the scope of the current study. From its geometrical position, we suggest two possibilities for the origin of the Chrystalls Beach Complex: (1) it represents a terrane subducted below the Caples before the amalgamation of the Caples and Rakaia Terranes; or (2) the Chrystalls Beach Complex is a channel of Rakaia-like sediments, which were underthrust below the Caples Terrane and entrained some Caples material either by erosion from the hanging wall or by pre-thrusting material flow (Fig. 9).

In the first scenario, it has not been established whether any material was accreted between deposition of the Caples Terrane and the arrival of the Rakaia Terrane. The Aspiring Lithological Association is situated between the Caples and Rakaia Terranes further northwest (Fig. 1), and may represent such a terrane. A link between the Aspiring Lithological Association and the Chrystalls Beach Complex was, however, rejected by Coombs et al. (2000) because of differences in metasediment geochemistry, and the sediment U/Pb zircon age patterns appear significantly different (Adams et al. 2007). A link has been proposed between the Chrystalls Beach Complex and the North Island Waipapa Terrane (Adams et al. 1999). Coombs et al. (2000) collated published geochemical analyses of Waipapa Terrane metasediments and compared these to data from the Chrystalls Beach Complex. The Waipapa Terrane sandstones are, in general, more mafic than Chrystalls Beach Complex greywacke (see discrimination diagrams in Coombs et al. 2000), and it is therefore unlikely that they were formed from the same source. On this basis, Coombs et al. (2000) rejected a connection between the Chrystalls Beach Complex and the Waipapa Terrane. Although future studies may reveal the presence of a terrane accreted between the Caples and the Rakaia Terranes, current data do not link the Chrystalls Beach Complex with other terranes geographically separating Caples and Rakaia.

If the mélange formed from subduction beneath the Caples Terrane, then some Caples material is likely to be eroded off the hanging wall and incorporated in the underthrust sediment pile (e.g., von Huene & Scholl 1991; von Huene et al. 2004). This would create an enigmatic sedimentary composition matching neither the overlying nor the subducting terrane. It would contain material from a sedimentary unit which was subducted rather than preserved and material scraped off the base of the Caples. In this model, the MORB pillow basalts at Taieri Mouth are

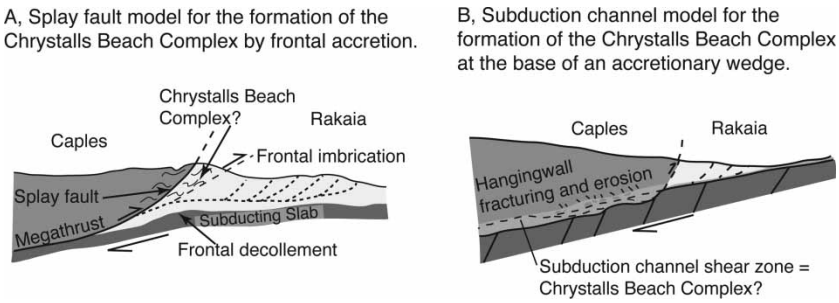

Fig. 9 Possible tectonic models for the formation of the Chrystalls Beach Complex: (A) megasplay thrust as inferred from seismological studies in many active margins (after Moore et al. 2007). The Chrystalls Beach Complex may represent such a shear zone separating the Caples and Rakaia Terranes. (B) A subduction channel is often inferred to be present within active megathrust shear zones, and may include material eroded from the base of the hanging wall (after von Huene et al. 2004). The Chrystalls Beach Complex could be a fossil example of such a channel from the Rangitata Orogeny.

interpreted as oceanic basement, on which the subducting (Rakaia?) sediments were deposited and transported. The fault-bounded blocks-in-matrix of OIB at Akatore Creek may be sheared-off segments of a subducted seamount, as commonly inferred in active margins (e.g., Cloos 1992).

There are two main possibilities for terrane superposition along a suture zone at an accretionary margin (Fig. 9): (1) a frontal accretion model where the landward section of the accretionary prism is thrust above a younger, outboard part of the wedge along a splay fault; and (2) a basal accretion model in which a proportion of the incoming sediment pile is subducted below the older, pre-existing, accretionary prism below the décollement. Both major splay faults and the décollement are major (likely) terrane-bounding structures, and both may be tabular shear zones containing trench-fill sediments.

In conclusion, the mixed-source rock assemblage in the Chrystalls Beach Complex could be part of the shear zone accommodating Caples-Rakaia collision in the Rangitata Orogeny. Such a shear zone is likely to have irregular boundaries, and the complex may be a thicker part of the shear zone and therefore outcrop within the overlying Caples Terrane. From compositional data alone, it is not possible to uniquely distinguish whether the shear zone is a splay fault within the New Zealand Mesozoic accretionary prism, or a subduction channel from below the décollement. It must also be noted that, as multiple basalt affinities are common throughout the Otago Schist, the Chrystalls Beach Complex is not necessarily very different from other parts of the schist. Several other rock assemblages within the schist may have a similar tectonic history to the Chrystalls Beach Complex.

Acknowledgements

Ray Marx assisted with fieldwork and provided helpful comments and discussion. We thank Damian Walls and Kat Lilly for assistance with XRF analyses, and Brent Pooley for sample preparation. J. Mike Palin provided discussion and assistance with LA-ICP-MS analyses, and Rick Sibson is thanked for discussion and comments on an early version of the manuscript. Reviews by Barry Roser and Nick Mortimer and the editorial assistance of Rob Lynch improved the final version of the paper. ÅF gratefully acknowledges support from a GNS Science Hazards Scholarship and a University of Otago Postgraduate Publishing Bursary.

References

Adams CJ, Robinson P 1993. Potassium-argon age studies of the metamorphism, uplift, and cooling in Haast Schist coastal sections south of Dunedin, Otago, New Zealand. New Zealand Journal of Geology and Geophysics 36: 317–325.

Adams CJ, Graham IJ 1997. Age of metamorphism of Otago Schist in eastern Otago and determination of protoliths from initial strontium isotope characteristics. New Zealand Journal of Geology and Geophysics 40: 275–286.

Adams CJ, Graham IJ, Johnston MR 1999. Age and isotopic characterisation of geological Terranes in Marlborough Schist, Nelson/Marlborough, New Zealand. New Zealand Journal of Geology and Geophysics 42: 33–55.

Adams CJ, Campbell HJ, Griffin WL 2007. Provenance comparisons of Permian to Jurassic tectonostratigraphic Terranes in New Zealand: perspectives from detrital zircon age patterns. Geological Magazine 144: 701–729.

Aita Y, Bragin N 1999. Non-Tethyan Triassic Radiolaria from New Zealand and northeastern Siberia. Geodiversitas (Earth Science Journal of the Natural History Museum of Paris) 21: 503–526.

Beccaluva L, Macciotta G, Piccardo GB, Zeda O 1989. Clinopyroxene compositions of ophiolite basalts as petrogenetic indicator. Chemical Geology 77: 165–182.

Bishop DG 1994. Geology of the Milton Area. Lower Hut, New Zealand, GNS Science.

Bishop DG, Turnbull IM 1997. Geology of the Dunedin area. Lower Hut, New Zealand, GNS Science.

Bradshaw JD, Adams CJ, Andrews PB 1981. Carboniferous to Cretaceous on the Pacific margin of Gondwana: the Rangitata phase of New Zealand. In: Cresswell MM, Vella P eds. Gondwana Five. Rotterdam, Netherlands. Pp. 217–221.

Breeding CM, Ague JJ 2002. Slab-derived fluids and quartz-vein formation in an accretionary prism, Otago Schist, New Zealand. Geology 30: 499–502.

Bucher K, Frey M 2002. Petrogenesis of Metamorphic Rocks. 7th Ed. Berlin, Springer-Verlag.

Campbell JK, Campbell JD 1970. Triassic tube fossils from Tuapeka rocks, Akatore, South Otago. New Zealand Journal of Geology and Geophysics 13: 392–399.

Cloos M 1992. Thrust-type subduction zone earthquakes and seamount asperities: A physical model for earthquake rupture. Geology 20: 601–604.

Coombs DS, Landis CA, Norris RJ, Sinton JM, Borns DJ, Craw D 1976. The Dun Mountain Ophiolite Belt, New Zealand, its tectonic setting, constitution, and origin, with special reference to the southern portion. American Journal of Science 276: 561–603.

Coombs DS, Landis CA, Hada S, Ito M, Roser BP, Suzuki T, Yoshikura S 2000. Geochemistry and Terrane correlation of the Chrystalls Beach-Brighton coastal block, southeast Otago, New Zealand. New Zealand Journal of Geology and Geophysics 43: 355–372.

Hada S, Yoshikura S, Aita Y, Sato K 1988. Notes on the geology and paleontology of the Chrystalls Beach Complex, South Island, New Zealand. Preliminary report on the accretion complex geology of Otago coast section in the South Island, New Zealand. Department of Geology, Kochi University, Japan. 21–28.

Hada S, Ito M, Landis CA, Cawood PA 2001. Large-scale translation of accreted Terranes along continental margins. Gondwana Research 4: 628–629.

Hay WW, Sloan JL, Wold CN 1988. Mass/age distribution and composition of sediments on the ocean floor and the global rate of sediment subduction. Journal of Geophysical Research 93: 14,933–14,940.

Howell DG, Murray RW 1986. A budget for continental growth and denudation. Science 233: 446–449.

Korsch RJ, Wellman HW 1988. The geological evolution of New Zealand and the New Zealand region. In: Nairn AEM, Stehli FG, Uyeda S eds. The Ocean Basins and Margins. London, Plenum Press. Pp. 411–482.

Landis CA, Campbell HJ, Aslund T, Cawood PA, Douglas A, Kimbrough DL, Pillai DDL, Raine JI, Willsman A 1999. Permian-Jurassic strata at Productus Creek, Southland, New Zealand: implications for Terrane dynamics of the eastern Gondwanaland margin. New Zealand Journal of Geology and Geophysics 42: 255–278.

Leterrier J, Maury RC, Thonon P, Girard D, Marchal M 1982. Clinopyroxene composition as a method of identification of the magmatic affinities of paleo-volcanic series. Earth and Planetary Science Letters 59: 139–154.

Ludden JN, Thompson G 1979. An evaluation of the behaviour of the rare earth elements during the weathering of sea-floor basalts. Earth and Planetary Science Letters 43: 85–92.

MacKinnon TC 1983. Origin of the Torlesse Terrane and coeval rocks, South Island, New Zealand. Geological Society of America Bulletin 94: 967–985.

Moore GF, Bangs NL, Taira A, Kuramoto S, Pangborn E, Tobin HJ 2007. Three-dimensional splay fault geometry and implications for tsunami generation. Science 318: doi:10.1126/science.1147195.

Morimoto N 1988. Nomenclature of pyroxenes. Mineralogical Magazine 52: 535–550.

Mortimer N 1993a. Geology of the Otago Schist and adjacent rocks. Lower Hutt, New Zealand, GNS Science.

Mortimer N 1993b. Jurassic tectonic history of the Otago Schist, New Zealand. Tectonics 12: 237–244.

Mortimer N 2000. Metamorphic discontinuities in orogenic belts: Example of the garnet-biotite-albite zone in the Otago Schist, New Zealand. International Journal of Earth Sciences 89: 295–306.

Mortimer N 2003. A provisional structural thickness map of the Otago Schist, New Zealand. American Journal of Science 303: 603–621.

Mortimer N 2004. New Zealand's Geological Foundations. Gondwana Research 7: 261–272.

Mortimer N, Roser BP 1992. Geochemical evidence for the position of the Caples-Torlesse boundary in the Otago Schist, New Zealand. Journal of the Geological Society (London) 149: 967–977.

Nelson KD 1982. A suggestion for the origin of mesoscopic fabric in accretionary mélange, based on features observed in the Chrystalls Beach Complex, South Island, New Zealand. Geological Society of America Bulletin 93: 625–634.

Nisbet GE, Pearce JA 1977. Clinopyroxene composition in mafic lavas from different tectonic settings. Contributions to Mineralogy and Petrology 63: 149–160.

Nishimura Y, Coombs DS, Landis CA, Itaya T 2000. Continuous metamorphic gradient documented by graphitization and K-Ar age, southeast Otago, New Zealand. American Mineralogist 85: 1625–1636.

Pearce JA 1996. A user's guide to basalt discrimination diagrams. In: Wyman DA ed. Trace Element Geochemistry of Volcanic Rocks: Applications to Massive Sulphide Exploration. Geological Association of Canada. 79–113.

Pearce JA 2008. Geochemical fingerprinting of oceanic basalts with applications to ophiolite classification and the search for Archean oceanic crust. Lithos 100: 14–48.

Pearce JA, Norry MJ 1979. Petrogenic implications of Ti, Zr, Y and Nb variations in volcanic rocks. Contributions to Mineralogy and Petrology 69: 33–47.

Robinson P 1958. Structural and metamorphic geology of the Brighton-Taieri Mouth area, East Otago, New Zealand. Unpublished MSc thesis, University of Otago.

Roser BP, Cooper AF 1990. Geochemistry and Terrane affiliation of Haast Schist from the western Southern Alps, New Zealand. New Zealand Journal of Geology and Geophysics 33: 1–10.

Roser BP, Korsch RJ 1999. Geochemical characterisation, evolution and source of a Mesozoic accretionary wedge: the Torlesse Terrane, New Zealand. Geological Magazine 136: 493–512.

Roser BP, Mortimer N, Turnbull IM, Landis CA 1993. Geology and geochemistry of the Caples Terrane, Otago, New Zealand: Compositional variations near a Permo-Triassic arc margin. In: Balance PF ed. South Pacific Sedimentary Basins. Amsterdam, Elsevier. Pp. 3–19.

Shervais JW 1982. Ti-V plots and the petrogenesis of modern ophiolitic lavas. Earth and Planetary Science Letters 59: 101–118.

Shervais JW, Kimbrough DL 1985. Geochemical evidence for the tectonic setting of the Coast Range ophiolite: a composite island arc-oceanic crust Terrane in western California. Geology 13: 35–38.

Sun SS, McDonough WF 1989. Chemical and isotopic systematics of oceanic basalts: implications for mantle composition and processes. In: Saunders AD, Norry MJ eds. Magmatism in the Ocean Basins. Geological Society of London Special Publication 42: Pp. 313–345.

Turnbull IM 2000. Geology of the Wakatipu Area. 1:250.000, GNS Science.

Underwood MB 2007. Sediment inputs to subduction zones: Why lithostratigraphy and clay mineralogy matters. In: Dixon TH, Moore JC eds. The Seismogenic Zone of Subduction Thrust Faults. New York, Colombia University Press. Pp. 42–86.

Vermeesch P 2006. Tectonic discrimination diagrams revisited. Geochemistry Geophysics Geosystems 7: doi:10.1029/2005GC001092.

von Huene R, Scholl DW 1991. Observations at convergent margins concerning sediment subduction, subduction erosion, and the growth of continental crust. Reviews of Geophysics 29: 279–316.

von Huene R, Ranero CR, Vannucchi P 2004. Generic model of subduction erosion. Geology 32: 913–916.

Winchester JA, Floyd PA 1977. Geochemical discrimination of different magma series and their differentiation products using immobile elements. Chemical Geology 20: 325–343.

Wood BL 1978. The Otago Schist megaculmination: Its possible origins and tectonic significance in the Rangitata Orogen of New Zealand. Tectonophysics 47: 339–368.

Yardley BWD 1982. The early metamorphic history of the Haast schists and related rocks of New Zealand. Contributions to Mineralogy and Petrology 81: 317–327.